Volume 8
Number 10
October 1969

# Inorganic Chemistry



CONTRIBUTION NO. 1548 FROM THE CENTRAL RESEARCH DEPARTMENT,
E. I. DU PONT DE NEMOURS AND COMPANY, EXPERIMENTAL STATION, WILMINGTON, DELAWARE 19898

## Structural and Bonding Characterizations of Molybdenum Dibromide, $Mo_6Br_{12}\cdot 2H_2O$

BY L. J. GUGGENBERGER AND A. W. SLEIGHT

*Received March 13, 1969*

Crystals of $Mo_6Br_{12}\cdot 2H_2O$ have been prepared by the reaction of molybdenum and hydrobromic acid at 700° and 3000 atm of pressure. The molecular and crystal structures of this compound have been determined from three-dimensional X-ray counter data. Crystals of the orange compound are tetragonal, space group I4/m, with cell dimensions of $a = 9.437 \pm 0.004$ Å and $c = 11.729 \pm 0.001$ Å. The calculated and observed densities are 4.992 and 4.995 g cm$^{-3}$, respectively. The structure has been refined by least squares to an $R$ value of 0.060. There are two discrete molecules of $Mo_6Br_{12}\cdot 2H_2O$ per cell. Each molecule consists of an octahedron of molybdenum atoms with bromine atoms bridging all of the octahedral faces and with four terminal, equatorial bromine ligands and two terminal, axial water ligands. Each molecule has the idealized $D_{4h}$ symmetry while the $Mo_6Br_8$ portion of the molecule has the idealized $O_h$ symmetry. Two Mo–Mo distances of 2.640 (2) and 2.630 (2) Å were observed. The bridging Mo–Br distances are 0.017 Å longer than the terminal distances. A valence bond description of the bonding is given for $Mo_6Br_{12}\cdot 2H_2O$. The extended Hückel molecular orbital procedure was used for molecular orbital calculations on $Mo_6Br_8^{4+}$ and $[Mo_6Br_8]Br_4\cdot 2H_2O$. Net overlap differences between atoms are reflected in the refined structure. Far-infrared and Raman data are presented.

### Introduction

The well-known $M_6X_8^{4+}$ metal atom cluster configuration is the precursor of a host of metal atom cluster compounds. The octahedral metal atom cluster compounds of the $M_6X_8^{4+}$ variety have been studied extensively with respect to their spectra[1-5] and bonding.[6-8] Although the gross structural features are known for compounds containing the $M_6X_8$ moiety, some of the most definitive structural parameters, such as the comparison of terminal and bridging M–X bond lengths, are not known accurately. This investigation was initiated to examine some of these structural parameters in greater detail. Review articles on metal atom cluster compounds and metal–metal bonds have appeared recently.[9-12]

The chemical stability of the $M_6X_8^{4+}$ species was demonstrated by Sheldon,[13] who prepared numerous compounds of the types $(Mo_6Cl_8)X_6^{2-}$ and $[Mo_6Cl_8]X_4L_2$ (X = Cl, Br, I, OH; L = $C_2H_5N$, $N(C_2H_5)_3$, $H_2O$) in which the $Mo_6Cl_8^{4+}$ grouping remained intact. The $Mo_6Cl_8^{4+}$ moiety was first characterized structurally by the X-ray work of Brosset on $[Mo_6Cl_8](OH)_4\cdot 14H_2O$ and $[Mo_6Cl_8](Cl_4\cdot 2H_2O)\cdot 6H_2O$.[14,15] The structure of $(NH_4)_2[Mo_6Cl_8]Cl_6\cdot H_2O$ was determined by Vaughan[16] by fitting a radial distribution function to the observed powder diffraction photograph. These structures established the correct over-all configuration but provided only very crude bond distances with the Mo–Mo and Mo–Cl distances varying from 2.62 to 2.69 Å and 2.43 to 2.62 Å, respectively. Recently Schäfer, *et al.*,[17] reported the structural characterization of molybdenum dichloride, $Mo_6Cl_{12}$, which contains the basic $Mo_6Cl_8$ unit linked to four similar units by bridging Cl atoms. A related structure occurs for $Nb_6I_{11}$ where a $Nb_3I_8^{3+}$ unit is linked by bridging I atoms to similar cluster units.[18]

In this work we are reporting the preparation, crystal structure, and bonding interpretation of $Mo_6Br_{12}\cdot 2H_2O$. This represents the first such characterization of a molybdenum dibromide and affords us accurate structural parameters for the discrete $Mo_6Br_{12}\cdot 2H_2O$ molecule.

(1) R. Mattes, *Z. Anorg. Allgem. Chem.*, **357**, 30 (1968).
(2) D. Hartley and M. J. Ware, *Chem. Commun.*, 912 (1967).
(3) F. A. Cotton, R. M. Wing, and R. A. Zimmerman, *Inorg. Chem.*, **6**, 11 (1967).
(4) R. J. H. Clark, D. L. Kepert, R. S. Nyholm, and G. A. Rodley, *Spectrochim. Acta*, **22**, 1697 (1966).
(5) F. A. Cotton and N. F. Curtis, *Inorg. Chem.*, **4**, 241 (1965).
(6) S. F. A. Kettle, *Theoret. Chim. Acta*, **3**, 211 (1965).
(7) F. A. Cotton and T. E. Haas, *Inorg. Chem.*, **3**, 10 (1964).
(8) L. D. Grossman, D. P. Olsen, and G. H. Duffey, *J. Chem. Phys.*, **38**, 73 (1963).
(9) M. C. Baird, *Progr. Inorg. Chem.*, **9**, 24 (1968).
(10) F. A. Cotton, *Quart Rev.* (London), **20**, 389 (1966).
(11) J. Lewis and R. S. Nyholm, *Sci. Progr.* (London), **52**, 557 (1964).
(12) H. Schäfer and H. G. Schnering, *Angew. Chem.*, **76**, 833 (1964).
(13) J. C. Sheldon, *J. Chem. Soc.*, 1007 (1960).
(14) C. Brosset, *Arkiv Kemi Mineral. Geol.*, **A20** (7), 1 (1945).
(15) C. Brosset, *ibid.*, **A22** (11), 1 (1946).
(16) P. A. Vaughan, *Proc. Natl. Acad. Sci. U. S.*, **36**, 461 (1950).
(17) H. Schäfer, H. G. Schnering, J. Tillack, F. Kuhnen, H. Wöhrle, and H. Baumann, *Z. Anorg. Allgem. Chem.*, **353**, 281 (1967).
(18) L. R. Bateman, J. F. Blount, and L. F. Dahl, *J. Am. Chem. Soc.*, **88**, 1082 (1966).

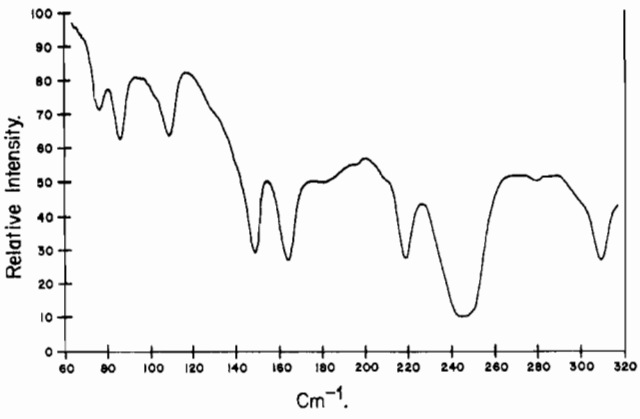


Figure 1.—Infrared spectrum of $Mo_6Br_{12}\cdot 2H_2O$ obtained using an interferometer.

## Experimental Section

**Synthesis.**—One gram of molybdenum and 1 ml of hydrobromic acid were sealed in a pressure-collapsible gold tube. This sealed ampoule was heated at 700° for 8 hr under 3000 atm of supporting pressure. The product consisted of crystals of molybdenum dioxide and molybdenum dibromide. The orange crystals of $Mo_6Br_{12}\cdot 2H_2O$ were easily separated by hand picking. High-purity molybdenum metal (99.95%) was obtained from Electronic Space Products, Inc.; the 48% hydrobromic acid was reagent grade.

*Anal.* Calcd for $Mo_6B_{12}\cdot 2H_2O$: Mo, 36.65; Br, 61.05; O, 2.04; H, 0.26. Found: Mo, 36.7; Br, 61.3; O, 2.1; H, 0.28.

The infrared spectrum of this compound in a fresh Nujol mull gave the characteristic water absorptions.

**Magnetic Susceptibility.**—The magnetic susceptibility of $Mo_6Br_{12}\cdot 2H_2O$ was measured by the conventional Faraday method using a Cahn RG microbalance and $HgCo(CNS)_4$ as a calibrant. A temperature-independent susceptibility of $-0.32 \times 10^{-3}$ emu/mol was found from 78 to 298°K. Similar values were found by Sheldon[13] for $[Mo_6Cl_8]Cl_4$, $(H_3O)_2[Mo_6Cl_8]Cl_6\cdot 6H_2O$, and $(NH_4)_2[Mo_6Cl_8]Cl_6\cdot H_2O$, *i.e.*, $-0.23$, $-0.36$, and $-0.24 \times 10^{-3}$ emu/mol, respectively. It should be noted that the usual diamagnetic corrections would change the sign of the susceptibility.

**Spectra.**—We examined the solid-state far-infrared and Raman spectra of $Mo_6Br_{12}\cdot 2H_2O$. The infrared spectrum below 320 $cm^{-1}$, recorded using an interferometer, is shown in Figure 1. The prominent peaks in Figure 1 are at 76, 86, 108, 148, 164, 219, 244 (vb), and 309 $cm^{-1}$. We observed five prominent peaks in the Raman spectrum at 211 (s), 179 (mw), 151 (w), 134 (ms), and 79 (s) $cm^{-1}$. Even a superficial analysis is complicated here since the species $[Mo_6Br_8]Br_4\cdot 2O$ (hydrogens omitted) of $D_{4h}$ point symmetry would be expected to have 13 infrared-active fundamentals ($5\ A_{2u} + 8\ E_u$) and 19 Raman-active fundamentals ($6\ A_{1g} + 3\ B_{1g} + 4\ B_{2g} + 6\ E_g$). In addition, we might expect an extensive mixing of symmetry-coordinate representations. The normal modes of the species $[Mo_6Br_8]Br_4\cdot 2O$ in the group $D_{4h}$ span the representation $6\ A_{1g} + 2\ A_{2g} + 3\ B_{1g} + 4\ B_{2g} + 6\ E_g + A_{1u} + 5\ A_{2u} + 2\ B_{1u} + 3\ B_{2u} + 8\ E_u$. The situation is simplified for a compound such as $[Mo_6Br_8]Br_6$ with $O_h$ point symmetry since there are only 5 infrared-active fundamentals ($5\ T_{1u}$) and 10 Raman-active fundamentals ($3\ A_{1g} + 3\ E_g + 4\ T_{2g}$). The infrared spectrum is included here because of the interest in normal-coordinate treatments on compounds of this type.[1,2]

**Crystal Data.**—Crystals of this compound are orange, tetragonal platelets usually exhibiting ten well-defined crystal faces of the {001} and {101} forms. The crystals are clearly optically uniaxial. The compound crystallizes in the tetragonal system with cell dimensions of $a = 9.437 \pm 0.004$ Å and $c = 11.729 \pm 0.001$ Å. These dimensions were obtained from a least-squares refinement of powder diffraction data recorded on a Hägg–Guinier camera using a KCl internal standard ($a_{25°} = 6.2931$ Å). The calculated density is 4.992 $g/cm^3$ corresponding to two $Mo_6Br_{12}\cdot 2H_2O$ molecules per cell. The density observed by the displacement method is 4.995 (5) $g/cm^3$.

Weissenberg and precession photographs showed the diffraction symmetry to be $C_{4h}$ with only the body-centering systematic extinction: $\{hkl\}$, $h + k + l = 2n + 1$. The possible space groups are I4/m, $I\bar{4}$, and I4. The space group I4/m proved to be the correct one (*vide infra*). For I4/m the equivalent general positions are $\pm[(x, y, z), (-x, -y, z), (-y, x, z), (y, -x, z) + (0, 0, 0), (1/2, 1/2, 1/2)]$.[19]

**Intensities.**—A crystal of dimensions $0.20 \times 0.20 \times 0.10$ mm was mounted with the $b$ axis coincident with the $\phi$ axis of a Picker four-circle diffractometer equipped with a scintillation detector and a pulse height discrimination. The data were collected using Zr-filtered Mo $K\alpha$ ($\lambda$ 0.7107 Å) radiation at a takeoff angle of 3.0°. The $\theta$–$2\theta$ scan technique was used with a scan speed of 1°/min. Individual backgrounds of 20 sec were measured before and after each scan. The scan length was 2° plus the angular separation of $K\alpha_1$ and $K\alpha_2$ for each reflection.

Only the 559 unique, symmetry-allowed reflections were measured in the range $0 < 2\theta \leq 50°$ except for $0kl$ and $h0l$ reflections which were both measured. The data were measured twice; the first set was rejected because we suspected that there were electronic fluctuations in the recording equipment while this data set was measured. Both sets of data were recorded and processed in the same manner.

The intensities were corrected for Lorentz–polarization effects in the usual way and for absorption using Prewitt's program ACACA.[20] The linear absorption coefficient for Mo $K\alpha$ radiation is 277 $cm^{-1}$ so there is a substantial absorption effect. The calculated transmission factors varied from 0.02 to 0.16 with the data well scattered throughout the range. We concluded on the basis of measuring equivalent reflections and examining the effect of crystal shape parameters on the transmission factors that the absorption correction was good to about 5% in $F$.

The errors in the intensities were estimated by $\sigma(I) = [CN + (t_c/2t_b)^2(BG_1 + BG_2) + (0.03I)^2]^{1/2}$, where CN is the total count measured in time $t_c$, $BG_1$ and $BG_2$ are the background counts each measured in time $t_b$, and $I$ is the integrated intensity after subtracting out the background. The $\sigma(F)$ was obtained from $\sigma(I)$ after the method of Williams[21,22] by $\sigma(F) = (LpT)^{-1/2}\cdot[(I + \sigma(I))^{1/2} - I^{1/2}]$, where $Lp$ is the Lorentz–polarization factor and $T$ the transmission factor. Structure factors for which $F$ was less than $\sigma(F)$ were called unobserved.

The atomic scattering factors used were those for neutral Mo, Br, and O.[23] Tabulated values[24] for the real and imaginary parts of the anomalous scattering of Mo and Br were used in including the anomalous dispersion effect in the calculated structure factors.

## Determination and Refinement of Structure

The first data set was used to calculate a three-dimensional Patterson function. A set of Mo atom positions was found consistent with the Patterson function. The remaining nonhydrogen atoms were located on an electron density difference map. The initial positional parameters were close to the final ones. The second data set was collected before the model was fully refined

(19) "International Tables for X-Ray Crystallography," Vol. I, The Kynoch Press, Birmingham, England, 1965, p 177.

(20) C. T. Prewitt, local unpublished computer programs, 1968. Additional programs used were the Busing–Levy ORFFE error function program, Johnson's ORTEP plotting program, and FOUR, a Fourier program written originally by Dr. C. J. Fritchie, Jr.

(21) D. E. Williams and R. E. Rundle, *J. Am. Chem. Soc.*, **86**, 1660 (1964).

(22) L. J. Guggenberger, *Inorg. Chem.*, **7**, 2260 (1968).

(23) H. P. Hansen, F. Herman, J. D. Lea, and S. Skillman, *Acta Cryst.*, **17**, 1040 (1964).

(24) "International Tables for X-Ray Crystallography," Vol. III, The Kynoch Press, Birmingham, England, 1962, p 215.

TABLE I
FINAL POSITIONAL AND THERMAL PARAMETERS FOR $Mo_6Br_{12} \cdot 2H_2O$

| Atom | Site symmetry | $x$ | $y$ | $z$ | $\beta_{11}$[a] | $\beta_{22}$ | $\beta_{33}$ | $\beta_{12}$ | $\beta_{13}$ | $\beta_{23}$ |
|---|---|---|---|---|---|---|---|---|---|---|
| $Mo_1$ | m | 0.1752 (1) | 0.0917 (1) | 0 | 0.0030 (2) | 0.0036 (2) | 0.0024 (1) | −0.0002 (1) | 0 | 0 |
| $Mo_2$ | 4 | 0 | 0 | 0.1580 (2) | 0.0038 (2) | $\beta_{11}$ | 0.0022 (2) | 0 | 0 | 0 |
| $Br_1$ | m | 0.4205 (2) | 0.2140 (2) | 0 | 0.0045 (2) | 0.0061 (2) | 0.0055 (2) | −0.0014 (2) | 0 | 0 |
| $Br_2$ | 1 | 0.0820 (1) | 0.2621 (1) | 0.1580 (1) | 0.0052 (2) | 0.0045 (2) | 0.0032 (1) | −0.0004 (1) | −0.0003 (1) | −0.0008 (1) |
| O | 4 | 0 | 0 | 0.3448 (16) | 0.0104 (16) | $\beta_{11}$ | 0.0034 (15) | 0 | 0 | 0 |

[a] The form of the anisotropic thermal ellipsoid is $\exp[-(\beta_{11}h^2 + \beta_{22}k^2 + \beta_{33}l^2 + 2\beta_{12}hk + 2\beta_{13}hl + 2\beta_{23}kl)]$. The estimated standard deviations of the least significant digits are given in parentheses. The refined value of the secondary extinction parameter is $C = 0.536 \times 10^{-5}$.

with the first set of data; hence, only the refinement using the second data set will be described in detail.

The refinement proceeded using the parameters determined with the first data set. The $R$ value, $\Sigma||F_o| - |F_c||/\Sigma|F_o|$, fell to 0.121 on varying the isotropic temperature factors and to 0.109 on varying the anisotropic temperature factors. At this point it was evident that the data suffered from secondary extinction since the $F_o$'s were much smaller than the $F_c$'s for the large $F$'s. A secondary extinction correction was applied after the method of Zachariasen[25] where the data are corrected according to $F_{cor} = F_o(1 + \beta C I_o)$. In this refinement $\beta$ was set equal to 1.0 for all reflections and $C$ was varied in the least-squares refinement.[26] We tried to obtain values of $\beta$ for each reflection after the method suggested by Zachariasen, but we were unable to get reasonable values, possibly because of the relatively large $\mu r$ involved. The reflections suffering most severely from secondary extinction ($\beta C I_o > 0.20$) were excluded from the refinement. The $R$ was 0.067 after three cycles of least-squares varying the scale factor, secondary extinction factor, and the positional and anisotropic thermal parameters. A separate refinement without the secondary extinction correction using those reflections suffering least from secondary extinction ($F_o < 250$) gave essentially identical positional parameters and even very similar thermal parameters to those obtained with the secondary extinction correction.

The question of the correct space group arises in the refinement. The question is pertinent with respect to constraints on the positional parameters and the ordering of the hydrogen atom positions of the two apical water molecules. It is possible for the nonhydrogen atoms to be in equivalent positions in all three space groups. To test this hypothesis we did separate refinements in the three possible space groups I4/m, I4, and $I\bar{4}$ excluding hydrogen atom positions in the structure factor calculations. There were 19 additional variables in the refinements in the I4 and $I\bar{4}$ space groups. In order for these refinements to be significant at the 0.50 level[27] (which is not very significant after all), there would have to be an improvement on the order of 5% in $wR$, where $wR$ is $\{\Sigma w(|F_o| - |F_c|)^2/\Sigma w|F_o|^2\}^{1/2}$. In our refinements in the I4 and $I\bar{4}$ space groups the $wR$ improved by only 4%. Thus we conclude that the I4/m space group adequately describes this structure at least as far as the heavy atoms are concerned.

Insofar as the hydrogen atom positions are concerned, they would have to be disordered in the space groups I4/m and I4, but they could be completely ordered in the space group $I\bar{4}$ giving a molecule of $D_{2d}$ point symmetry. The hydrogen atom disorder would presumably be of the form of a stacking disorder wherein individual molecules with ordered hydrogen atom positions are stacked next to molecules with waters rotated by 90° so that the over-all space group symmetry is I4/m. In view of the results of our statistical comparison of the refinements in I4/m, I4, and $I\bar{4}$, we conclude that I4/m is the correct space group with the water molecules randomly disordered between two energetically equivalent sites. We did look at the final electron density difference map in the region of the hydrogen atom positions but we did not feel justified in assigning any of the small peaks in this region to hydrogen atom positions.

The final refinements were carried out in the space group I4/m. The final refined parameters are given in Table I. The observed and calculated structure factors are given in Table II where an asterisk following a reflection is used to denote an unobserved reflection and an E is used to denote a reflection excluded because of the large secondary extinction effect. The final $R$ factors for observed reflections were 0.060 and 0.065 for $R$ and $wR$, respectively. The corresponding $R$ and $wR$ for all the data were 0.075 and 0.079, respectively. The maximum peak in the final electron density difference map was 1.4 $e^-/Å^3$. The standard deviation of an observation of unit weight was 1.83.

## Description of the Structure

The crystal structure consists of the body-centered packing of discrete molecules of $Mo_6Br_{12} \cdot 2H_2O$. One of these molecules, the hydrogen atoms omitted, is depicted in Figure 2. This molecule may be described as an octahedron of Mo atoms with Br atoms bridging all of the octahedral faces and with terminal, equatorial Br ligands and terminal, axial $H_2O$ ligands. Alternatively the cluster portion of this structure, $Mo_6Br_8^{4+}$, may be described as a cube of Br atoms with Mo atoms in the face-centered positions.

The molecular packing of this structure is shown clearly in Figures 3 and 4, again with the H atoms omitted. In both figures the octahedra of metal atoms have

(25) W. H. Zachariasen, *Acta Cryst.*, **16**, 1139 (1963).
(26) C. T. Prewitt and R. D. Shannon, *ibid.*, **B24**, 869 (1968).
(27) W. C. Hamilton, *ibid.*, **18**, 502 (1965).

TABLE II

OBSERVED AND CALCULATED STRUCTURE FACTORS FOR $Mo_6Br_{12}\cdot 2H_2O$

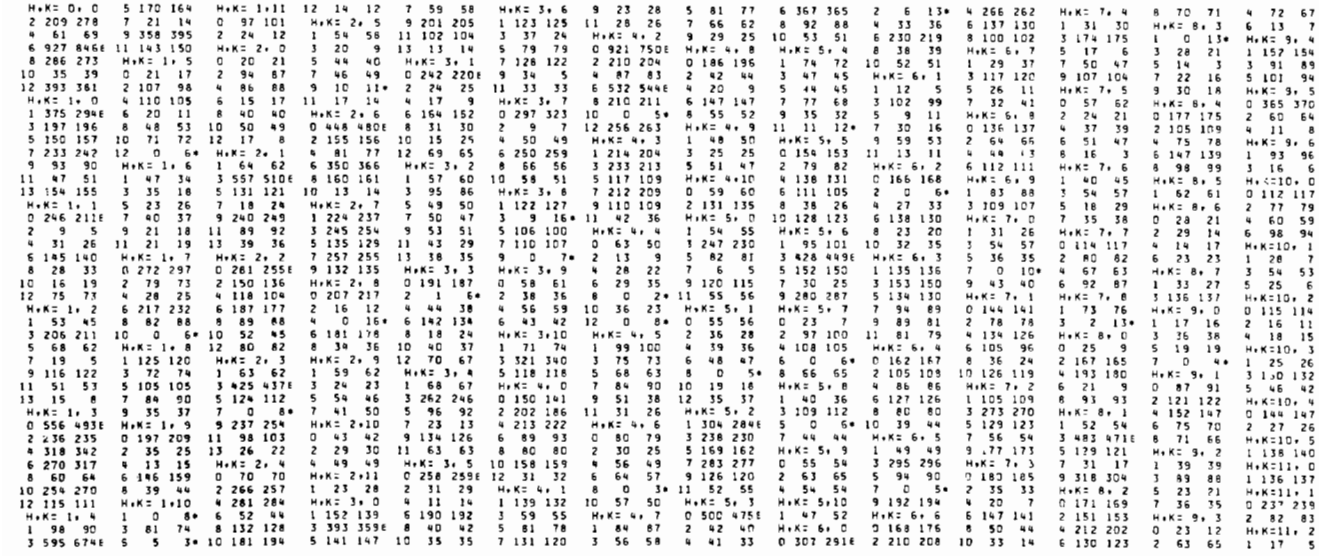

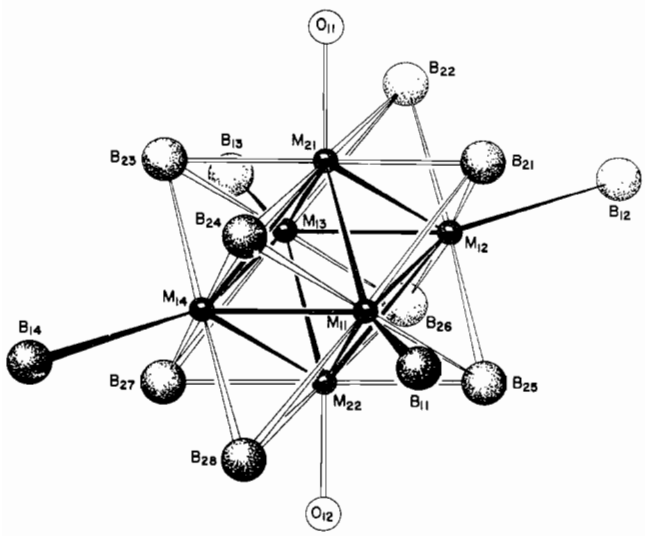


Figure 2.—The molecular configuration of $[Mo_6Br_8]Br_4\cdot 2H_2O$. The molybdenum, bromine, and oxygen atoms are labeled by M's, B's, and O's, respectively.

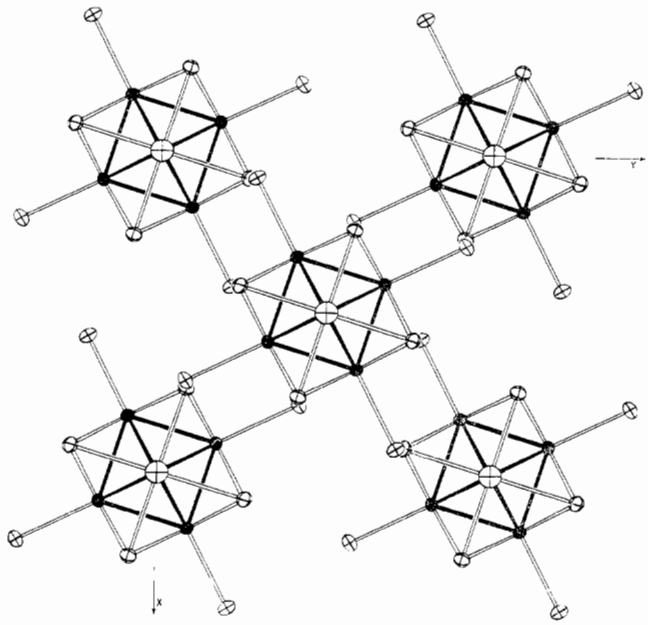

Figure 3.—A view of the crystal structure of $[Mo_6Br_8]Br_4\cdot 2H_2O$ down the $c$ axis. The center molecule is translated by $^1/_2c$.

been blackened for emphasis. Figure 3 shows a picture of this structure as viewed down the $c$ axis illustrating how the packing in the $ab$ plane is determined primarily by the packing requirements of the terminal Br atoms. Figure 4 shows the structure viewed down the $a$ axis. The shortest nonhydrogen intermolecular contacts are given in Table III; there are no unusual intermolecular interactions. The holes for the water hydrogen atoms are evident in Figure 4. There is enough room for the two adjacent water molecules along the $c$ axis to be eclipsed. However, for a given molecule there are two energetically equivalent positions (separated by a 90° rotation about $c$) for the water hydrogen atoms so that we would expect two adjacent water molecules to assume the staggered configuration. A given water molecule then chooses one of the two equivalent orientations and the water on the adjacent cluster assumes the other orientation; the same considerations apply to both waters on a given cluster. The result is a random distribution of waters between the two equivalent orientations.

TABLE III

INTERMOLECULAR DISTANCES (Å)[a]

| | | | |
|---|---|---|---|
| $Br_{24}$–$Br_{13}'$ | 3.736 (2) | $Br_{21}$–$Br_{27}''$ | 3.842 (2) |
| $Br_{14}$–$Br_{13}'$ | 3.961 (2) | $Br_{21}$–$Br_{26}''$ | 3.992 (2) |
| $Br_{11}$–$O_{12}''$ | 3.341 (10) | | |

[a] Standard deviations are given in parentheses. The primed and double-primed atoms are related to those in Table I by $(x+1, y, z)$ and $(^1/_2+x, ^1/_2+y, ^1/_2+z)$, respectively.

The atoms in Figure 2 are labeled so that the first digit of the subscript identifies the atom type and the second digit identifies sequentially the atoms of a given type. The unique intramolecular distances and angles are given in Tables IV and V, respectively; the thermal

corrections to the distances are included in Table IV for two vibration models.[28] The distances and angles in braces are chemically, but not crystallographically, equivalent. It is clear from inspection of the distances and angles that the molecule has the idealized $D_{4h}$ symmetry and the $Mo_6Br_8$ moiety has the idealized $O_h$ symmetry. Distances and angles not specifically given in Tables IV and V are related to those given by the space group imposed $C_{4h}$ symmetry of the molecule.

TABLE IV
SELECTED INTRAMOLECULAR DISTANCES (Å) FOR $Mo_6Br_{12}\cdot 2H_2O$[a]

| | | Corrections | |
|---|---|---|---|
| | | Riding motion | Ind motion |
| $Mo_{11}$–$Mo_{12}$ | 2.640 (2) | +0.000 | +0.012 |
| $Mo_{11}$–$Mo_{21}$ | 2.630 (2) | +0.001 | +0.013 |
| $Mo_{11}$–$Br_{21}$ | 2.606 (2) | +0.004 | +0.015 |
| $Mo_{11}$–$Br_{24}$ | 2.606 (2) | +0.004 | +0.015 |
| $Mo_{21}$–$Br_{21}$ | 2.591 (2) | +0.003 | +0.016 |
| $Mo_{11}$–$Br_{11}$ | 2.587 (2) | +0.007 | +0.019 |
| $Mo_{21}$–$O_{11}$ | 2.191 (18) | +0.01 | +0.03 |
| $Br_{11}$–$Br_{21}$ | 3.721 (2) | | |
| $Br_{11}$–$Br_{24}$ | 3.671 (2) | | |
| $Br_{21}$–$Br_{22}$ | 3.665 (2) | | |
| $Br_{21}$–$Br_{25}$ | 3.706 (3) | | |
| $Br_{21}$–$O_{11}$ | 3.393 (12) | | |

[a] The standard deviations of the least significant digits are given in parentheses. The thermal motion corrections to the bond lengths are for the cases where the second atom is assumed to ride on the first (riding motion) and where the two atoms move independently (ind motion).

TABLE V
INTERATOMIC ANGLES FOR $Mo_6Br_{12}\cdot 2H_2O$ (DEG)[a]

| | | | |
|---|---|---|---|
| $Mo_{12}$–$Mo_{11}$–$Mo_{21}$ | 59.88 (2) | $Br_{21}$–$Mo_{11}$–$Br_{25}$ | 90.64 (7) |
| | | $Br_{24}$–$Mo_{11}$–$Br_{28}$ | 90.64 (7) |
| $Mo_{21}$–$Mo_{11}$–$Mo_{22}$ | 89.58 (8) | $Mo_{11}$–$Mo_{21}$–$Mo_{13}$ | 90.41 (8) |
| $Mo_{21}$–$Mo_{11}$–$Br_{11}$ | 135.20 (4) | $Mo_{11}$–$Mo_{21}$–$Mo_{12}$ | 60.24 (4) |
| $Br_{21}$–$Mo_{11}$–$Br_{24}$ | 89.34 (6) | $Mo_{11}$–$Mo_{21}$–$O_{11}$ | 134.79 (4) |
| $Br_{21}$–$Mo_{11}$–$Br_{28}$ | 178.50 (6) | $Br_{21}$–$Mo_{21}$–$O_{11}$ | 90.00 (5) |
| $Mo_{21}$–$Mo_{11}$–$Br_{21}$ | 59.32 (4) | $Mo_{11}$–$Mo_{21}$–$Br_{21}$ | 59.88 (4) |
| $Mo_{21}$–$Mo_{11}$–$Br_{24}$ | 59.32 (4) | $Mo_{11}$–$Mo_{21}$–$Br_{24}$ | 59.88 (4) |
| $Mo_{12}$–$Mo_{11}$–$Br_{21}$ | 59.58 (5) | $Mo_{11}$–$Br_{21}$–$Mo_{12}$ | 60.85 (5) |
| $Mo_{14}$–$Mo_{11}$–$Br_{24}$ | 59.57 (5) | $Mo_{11}$–$Br_{21}$–$Mo_{21}$ | 60.80 (5) |
| | | $Mo_{12}$–$Br_{21}$–$Mo_{21}$ | 60.80 (5) |

[a] The standard deviations of the least significant digits are given in parentheses.

In the $Mo_6Br_{12}\cdot 2H_2O$ cluster we expect to find two types of Mo–Mo distances ($Mo_{11}$–$Mo_{12}$, $Mo_{11}$–$Mo_{21}$) and three types of Mo–Br distances ($Mo_{11}$–$Br_{11}$, $Mo_{11}$–$Br_{21}$, $Mo_{21}$–$Br_{21}$). In the case of the isolated $O_h$ symmetry clusters $Mo_6Br_8^{4+}$ and $[Mo_6Br_8]Br_6^{2-}$ there would be only one Mo–Mo distance and two Mo–Br distances ($Mo_{11}$–$Br_{11}$, $Mo_{11}$–$Br_{21}$). The relationship between terminal and bridging Br's will be discussed in greater detail in the next section on bonding.

Observed Mo–Mo bonds vary considerably between 2.50 and 2.93 Å.[9] The Mo–Mo distance in the metal is 2.725 Å.[29] The Mo–Mo distances in $Mo_6$ clusters, however, would not be expected to vary greatly from cluster

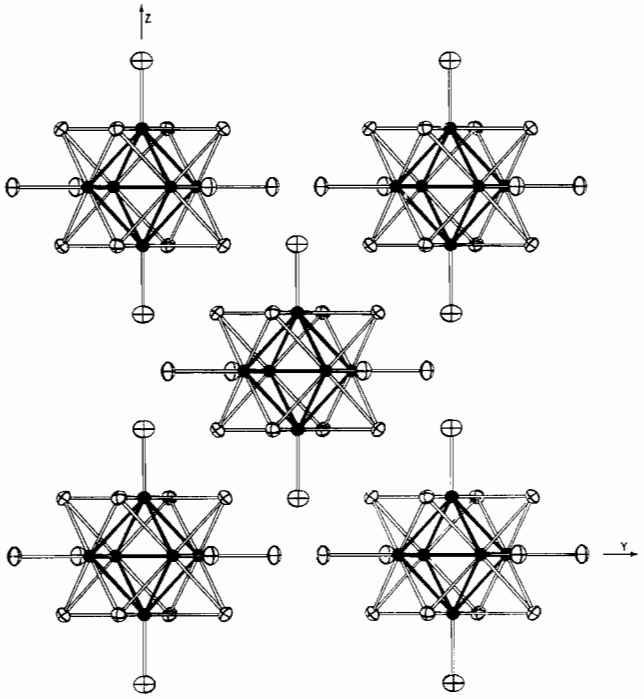


Figure 4.—A view of the crystal structure of $[Mo_6Br_8]Br_4\cdot 2H_2O$ down the $a$ axis. The center molecule is translated by $^1/_2a$

to cluster and this is, in fact, what is observed with distances close to the "expected" Mo–Mo single-bond distance of 2.59 Å.[30] The early work on $(NH_4)_2[Mo_6Cl_8]Cl_6\cdot H_2O$,[16] $[Mo_6Cl_8](Cl_4\cdot 2H_2O)\cdot 6H_2O$,[15] and $[Mo_6Cl_8](OH)_4\cdot 14H_2O$[14] gave Mo–Mo distances between 2.62 and 2.69 Å, but the accuracy of that work is not sufficient to compare it critically with this work. In the recent work on $\{[Mo_6Cl_8]Cl_2\}Cl_{4/2}$[17] the Mo–Mo bonds were found to be equal within the accuracy of the determination at 2.61 ± 0.01 Å. The Mo–Mo distances of 2.630 (2) and 2.640 (2) Å observed in the $Mo_6Br_{12}\cdot 2H_2O$ structure are not very different in an absolute sense, but they are significantly different in view of the errors involved. The maximum observed difference between the terminal and bridging Mo–Br distances is 0.019 Å. This can be contrasted with the geometry of the $Re_3Cl_{12}^{3-}$ anion[31] where the Re atom occupies a position similar to the Mo in $Mo_6Br_{12}\cdot 2H_2O$ but where the terminal Re–Cl distance is 0.14 Å longer than the other four. We believe the Mo–Mo and Mo–Br bonds both have bond orders close to 1; also, we believe the small differences in the Mo–Mo and Mo–Br bond lengths are real and result from net bonding effects. This will be discussed in greater detail in the next section.

The Mo–O bonds observed to date vary from about 1.7 to 2.4 Å corresponding to different bond orders. The Mo–O distance of 2.19 Å observed here is shorter than other observed Mo–O ($H_2O$) distances of 2.33[32] and

(28) W. R. Busing and H. A. Levy, *Acta Cryst.*, **17**, 142 (1964).
(29) "Tables of Interatomic Distances and Configuration in Molecules and Ions," Special Publication No. 18, The Chemical Society, London, 1965, p S7s.
(30) L. Pauling, "The Nature of the Chemical Bond," 3rd ed, Cornell University Press, Ithaca, N. Y., 1960, p 440.
(31) J. A. Bertrand, F. A. Cotton, and W. A. Dollase, *Inorg. Chem.*, **2**, 1166 (1963).
(32) F. A. Cotton, S. M. Morehouse, and J. S. Wood, *ibid.*, **3**, 1603 (1964).

2.39 Å.[33] The Mo–O distance here is equivalent, however, to single-bonded Mo–O distances where the O is a carboxylate oxygen.[34] This shortening can be easily rationalized in terms of increased oxygen participation with the extensive delocalized bonding within the metal atom cluster.

### Bonding in $Mo_6Br_8^{4+}$ and $[Mo_6Br_8]Br_4 \cdot 2H_2O$

The bonding in the $Mo_6Br_{12} \cdot 2H_2O$ structure can be described reasonably well in terms of the valence-bond language. The representation spanned by the nine bonds to Mo in the $C_{4v}$ symmetry group is: $3\,A_1 + B_1 + B_2 + 2\,E$. However, this is precisely the representation spanned by the nine atomic orbitals of Mo most likely to be involved in bonding, *i.e.*, 5s, 5p, 4d. Thus, for a given Mo atom there are atomic orbitals which can hybridize to give orbitals of the proper symmetry to bond to one terminal water or Br ligand, four Mo atoms, and four bridging Br atoms. The localized bonding is summarized in Table VI. Insofar as the over-all cluster is concerned the "magic number" of 84 electrons is contributed to form the 42 bonds involved in bonding to and within the cluster. Thus the valence-bond interpretation of localized single bonds works out rather well in this case. There are, however, serious drawbacks to this description. For example, it requires unreasonably bent bonds between the Mo atoms and the bridging Br atoms which presumably use p orbitals in bonding.[35] Also it does not easily account for the subtle, but important, structural features such as differences in bond lengths and charge distributions.

TABLE VI

VALENCE-BOND DESCRIPTION OF BONDING IN $Mo_6Br_{12} \cdot 2H_2O$

| Bond types | Symmetries of local bonds | Symmetries of Mo atomic orbitals: $A_1$ | $B_1$ | $B_2$ | E |
|---|---|---|---|---|---|
| 1 Mo–$H_2O$ or Mo–Br | $A_1$ | $5p_z$ | | | |
| 4 Mo–Mo | $A_1 + B_1 + E$ | $4d_{z^2}$ | $4d_{x^2-y^2}$ | | $(4d_{xz}, d_{yz})$ |
| 4 Mo–Br | $A_1 + B_2 + E$ | 5s | | $4d_{xy}$ | $(5p_x, p_y)$ |

Semiquantitative molecular orbital descriptions of the bonding in the $Mo_6X_8^{4+}$ cluster have been given by Crossman, *et al.*,[8] and Kettle.[6] Cotton and Haas[7] have described the bonding in the $Mo_6X_8^{4+}$ cluster more quantitatively. The Cotton and Haas (CH) model of the bonding in $Mo_6X_8^{4+}$ will be described in terms of the $Mo_6Br_8^{4+}$ portion of the structure shown in Figure 2 since it pertains to the calculations we are reporting. The CH model makes use of the fact that each Mo atom lies at the center of a square $MoBr_4$ group. Incidentally, our work proves that this $MoBr_4$ group is really planar. The metal–metal bonding and metal–bromine bonding are separated by using $4d_{xy}$, 5s, $5p_x$, and $5p_y$ Mo orbitals to bond to the bridging Br's and $4(d_{z^2}, d_{xz}, d_{yz}$, and $d_{xy})$ Mo orbitals for the Mo$_6$ metal–metal bonding. A terminally directed $5p_z$ Mo orbital is used to bond to an additional ligand (Br or $H_2O$ in our case); they assume that the Mo $4d_{z^2}$ and $5p_z$ orbitals do not hybridize. Slater atomic orbital (AO) wave functions are used to describe the Mo d orbitals and a molecular orbital (MO) calculation gives the 24 MO's describing the Mo–Mo bonding in the $Mo_6$ cluster. The off-diagonal Hückel matrix elements are taken proportional to the appropriate overlap with the sign reversed.

In the CH scheme ligand effects are completely ignored. In the substituted $Mo_6X_8^{4+}$ clusters, such as the $[Mo_6Br_8]Br_4 \cdot 2H_2O$ structure reported here, the ligand effects and their relation to the metal–metal bonding are of interest. Also the CH method of separating out the bonding contributions does not lend itself well to examining quantities which are dependent on net bonding effects such as net overlap populations.

Therefore, we decided to reinvestigate the bonding in $Mo_6Br_8^{4+}$, this time including ligand effects. After this was done, the plan was to use the parameters determined in the $Mo_6Br_8^{4+}$ calculation to examine the effect on the $Mo_6Br_8^{4+}$ cluster of adding terminal ligands, thus examining the bonding in the $[Mo_6Br_8]Br_4 \cdot 2H_2O$ structure. The extended Hückel molecular orbital approach which includes all interatomic interactions was used in this work.[36]

The basis set of 86 AO's used in the LCAO–MO approximation in the $Mo_6Br_8^{4+}$ cluster calculation consisted of 54 valence AO's of Mo (5s, 5p, 4d) and 32 valence AO's of Br (4s, 4p). The basis set in the $[Mo_6Br_8]Br_4 \cdot 2H_2O$ calculation consisted of the preceding plus 16 additional Br AO's, 8 oxygen AO's (2s, 2p), and 4 H AO's (1s). The AO's were expressed as Slater-type orbitals.[37] The off-diagonal matrix elements were evaluated using the Wolfsberg–Helmholz[38] approximation

$$H_{ij} = KS_{ij}(H_{ii} + H_{jj})/2$$

with $K = 1.75$. All overlap integrals are explicitly calculated in this approach.

We assumed the idealized $O_h$ geometry for the $Mo_6Br_8^{4+}$ cluster taking a cube of Br atoms with the Mo atoms in the face-centered positions. The dimensions were determined to make the Mo–Mo distance equal to 2.635 Å, the average of the two Mo–Mo distances observed. The Mo–Br distances then for this cluster were also 2.635 Å. The idealized geometry was used so as not to bias the calculation in favor of the effects we intended to seek. The coordinate system used had the origin at the center of the octahedron (Figure 2) with $x$, $y$, and $z$ directed at $Mo_{11}$, $Mo_{12}$, and $Mo_{21}$, respectively.

The initial Mo, Br, and O orbital exponents ($\zeta$) were taken from Clementi's tabulated values which were optimized in a minimal basis set self-consistent-field

(33) J. G. Scane, *Acta Cryst.*, **23**, 85 (1967).

(34) J. J. Park, M. D. Glick, and J. L. Hoard, *J. Am. Chem. Soc.*, **91**, 301 (1969).

(35) R. J. Gillespie in "Advances in the Chemistry of the Coordination Compounds," S. Kirschner, Ed., The Macmillan Co., New York, N. Y., 1961, p 41.

(36) R. Hoffman, *J. Chem. Phys.*, **39**, 1397 (1963). The program used was a local modification of a program written by R. Hoffman.

(37) J. C. Slater, *Phys. Rev.*, **36**, 57 (1930).

(38) M. Wolfsberg and L. Helmholz, *J. Chem. Phys.*, **20**, 837 (1952).

calculation.[39,40] The Slater exponent[37] was used for H. The Mo (5p) orbital was assumed to be slightly more diffuse than the Mo (5s) orbital. The initial values of the diagonal Hamiltonian matrix elements were chosen in the usual way as the negative of the valence state ionization potentials (VSIP). The initial values for Mo and Br were calculated from the spectral data given by Moore.[41] The values for O were taken from Basch, *et al.*[42] These data are summarized in Table VII.

TABLE VII
ORBITAL EXPONENTS AND VALENCE-STATE IONIZATION ENERGIES

| | Initial parameters | | Final parameters | |
|---|---|---|---|---|
| Orbital | $\zeta$ | $-H_{ii}$, eV | $\zeta$ | $-H_{ii}$, eV |
| Mo (5s) | 1.22 | 7.10 | ... | 8.36 |
| Mo (5p) | 1.10 | 3.92 | ... | 5.18 |
| Mo (4d) | 2.85 | 8.56 | 1.80 | 9.84 |
| Br (4s) | 2.64 | 23.80 | ... | ... |
| Br (4p) | 2.26 | 11.84 | ... | ... |
| O (2s) | 2.25 | 32.33 | ... | ... |
| O (2p) | 2.23 | 15.79 | ... | ... |
| H (1s) | 1.00 | 13.60 | ... | ... |

The MO's of interest involve bonding primarily of the metal d orbitals so that the Mo (4d) orbital exponents and VSIP's for the Mo orbitals are very important. We "optimized" these quantities by first varying the orbital exponents holding the VSIP's constant at their initial values and then varying the VSIP's holding the orbital exponents fixed. We felt the exponent of 2.85 would be the upper limit for the Mo (4d) orbital. The exponent using Slater's rules[37] is about 1.3, the actual number depending on the configuration assumed. We felt this would be a lower limit for reasons discussed by Cotton and Haas.[7] Accordingly we calculated sets of molecular orbitals varying the Mo (4d) exponent between 1.50 and 2.85. The results are shown in Figure 5 where only the highest bonding and lowest antibonding MO's are shown. Specifically, the orbitals shown are those with large Mo (4d) orbital contributions, *i.e.*, those involved primarily in Mo–Mo bonding. The representation spanned by the 30 Mo d orbitals in the $O_h$ point group is

$$A_{1g} + A_{2g} + A_{2u} + 2\,E_g + E_u + T_{1g} + 2\,T_{2g} + 2\,T_{1u} + 2\,T_{2u}$$

An interesting feature of the calculation was the variation of the total energy as a function of the orbital exponents. The total energy showed a definite minimum at a Mo (4d) exponent value of 1.80. The energy curve was parabolic in the region of the minimum. We originally guessed that 2.0 would be a good exponent value to describe the Mo (4d) orbitals, but in view of the definite energy minimum at 1.80, we chose this value for our self-consistent-charge iterative calculation. The

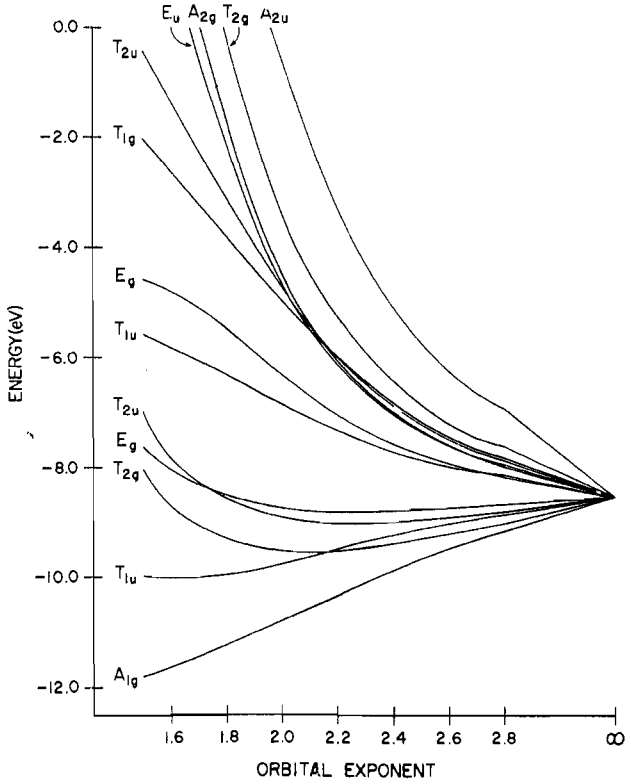


Figure 5.—The variation of the Mo–Mo bonding molecular orbitals as a function of the Mo (4d) orbital exponent.

net atom charges based on the original input $H_{ii}$'s and an exponent of 1.80 were +1.03 for Mo and −0.27 for Br.

We then varied the $H_{ii}$'s for Mo until the output Mo charge matched the input Mo charge to within 0.02. We used a 0.75-eV change in $H_{ii}$ per unit of change in positive charge in order to get convergence in this procedure. We assumed that the shielding parameters would not change with the charge distribution. The final $H_{ii}$'s are given in Table VII. The final net atom charges were +0.64 for Mo and +0.02 for Br. The Br charge of +0.02 results in part from the method which tends to minimize charge differences, but remember also that the cluster has a +4 charge. The final MO distribution for the MO's involved primarily in Mo–Mo bonding is given in Figure 6.

As in the CH calculation all of the bonding MO's and none of the antibonding MO's are filled with a gap energy of 2.1 eV. The origin of the Mo–Mo bonding in $Mo_6Br_8^{4+}$ can be seen in Table VIII which gives the Mulliken population analysis[43] for the AO's involved in bonding. The analysis given is specifically for the bonding of the axial Mo ($Mo_{21}$ in Figure 2) to its bonded atoms. Of course, the other Mo atoms are equivalent by symmetry to $Mo_{21}$ so that the overlap populations involving these atoms to their adjacent atoms are the same except that different AO's will be involved. The net overlap populations are 0.341 for Mo–Mo and 0.348 for Mo–Br. We take this as an indication that the

(39) E. Clementi and D. L. Raimondi, *J. Chem. Phys.*, **38**, 2686 (1963).
(40) E. Clementi, D. L. Raimondi, and W. P. Reinhardt, *ibid.*, **47**, 1300 (1967).
(41) C. E. Moore, "Atomic Energy Levels," U. S. National Bureau of Standards Circular 167, U. S. Government Printing Office, Washington, D. C., 1949 and 1952.
(42) H. Basch, A. Viste, and H. B. Gray, *Theoret. Chim. Acta*, **3**, 458 (1965).
(43) R. S. Mulliken, *J. Chem. Phys.*, **23**, 1883 (1955).

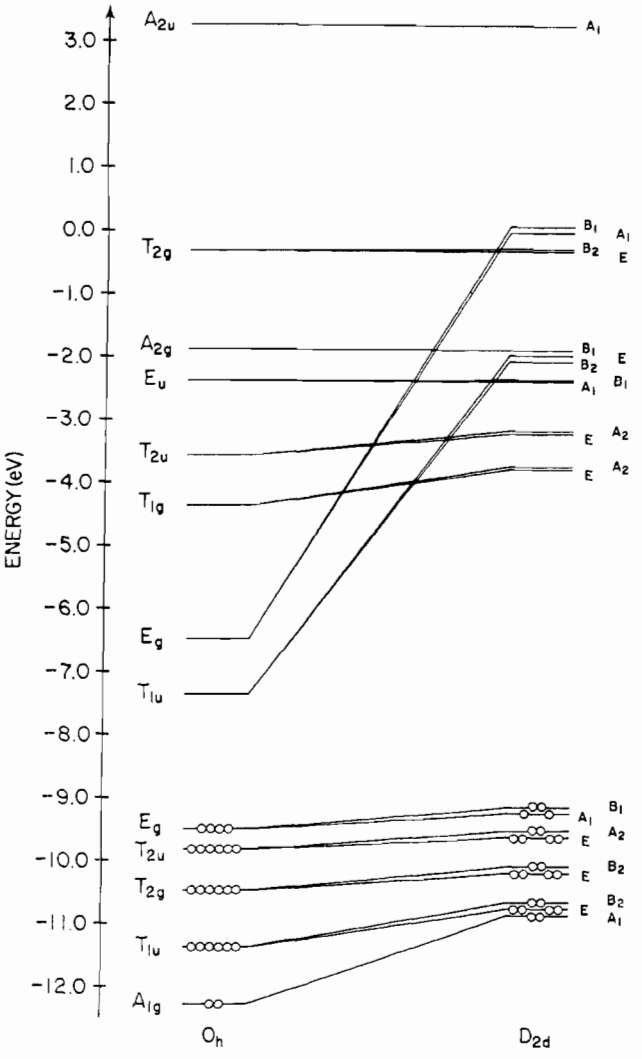


Figure 6.—The energy level diagrams for $Mo_6Br_8^{4+}$ on the left and $[Mo_6Br_8]Br_4 \cdot 2H_2O$ on the right. Only those molecular orbitals involved primarily in Mo–Mo bonding are shown.

TABLE VIII

OVERLAP POPULATIONS FOR ATOMIC ORBITALS INVOLVED IN Mo–Mo BONDING IN $Mo_6Br_8^{4+}$ [a]

| | | $Mo_{21}$ | | | | |
|---|---|---|---|---|---|---|
| | | $d_{z^2}$ | $d_{xz}$ | $d_{x^2-y^2}$ | $d_{yz}$ | $d_{xy}$ |
| $Mo_{11}$ and $Mo_{13}$ | $d_{z^2}$ | 0.0522 | 0.0095 | 0.0804 | 0.0000 | 0.0000 |
| | $d_{xz}$ | 0.0075 | 0.1142 | 0.0265 | 0.0000 | 0.0000 |
| | $d_{x^2-y^2}$ | 0.0122 | 0.0244 | 0.0004 | 0.0000 | 0.0000 |
| | $d_{yz}$ | 0.0000 | 0.0000 | 0.0000 | −0.0006 | −0.0038 |
| | $d_{xy}$ | 0.0000 | 0.0000 | 0.0000 | 0.0379 | −0.0006 |
| $Mo_{12}$ and $Mo_{14}$ | $d_{z^2}$ | 0.0522 | 0.0000 | 0.0804 | 0.0095 | 0.0000 |
| | $d_{xz}$ | 0.0000 | −0.0006 | 0.0000 | 0.0000 | −0.0038 |
| | $d_{x^2-y^2}$ | 0.0122 | 0.0000 | 0.0004 | 0.0244 | 0.0000 |
| | $d_{yz}$ | 0.0075 | 0.0000 | 0.0265 | 0.1142 | 0.0000 |
| | $d_{xy}$ | 0.0000 | 0.0379 | 0.0000 | 0.0000 | −0.0006 |

[a] The local coordinate system is the same for all atoms with $x$, $y$, and $z$ coincident with the position vectors from the center of the cage to atoms $Mo_{11}$, $Mo_{12}$, and $Mo_{21}$, respectively.

bond orders are similar for the Mo–Mo and Mo–Br bonds.

On comparing our calculation with the CH calculation we see that their approximation of excluding Mo ($d_{xy}$) in their metal–metal bonding scheme is a good one (see Table VIII). There are significant ligand contributions, however, to the MO's involved in the Mo–Mo bonding. Our MO diagram in Figure 5 is similar to the CH diagram when the different coordinate systems are taken into account. Our bonding $E_g$ and $T_{2u}$ levels are interchanged with respect to the CH model. This might result from ligand effects since for our Mo–Mo bonding MO's the $E_g$ level has the largest Br contributions and these are of an antibonding nature raising the energy of this MO. At a $\zeta$ of 1.80 we are close to the crossover between the $E_g$ and $T_{2u}$ levels; this crossover in the CH calculation is at much higher $\zeta$ values.[44] Certainly the nature of the highest bonding MO is important with respect to possible oxidations of the cluster. The MO's involving primarily Mo–Br bonding are still lower in energy than those depicted in Figures 4 and 5.

The "optimized" parameters obtained from the $Mo_6Br_8^{4+}$ calculation were then used in a MO calculation on $[Mo_6Br_8]Br_4 \cdot 2H_2O$. The geometry assumed was the idealized geometry used in the $Mo_6Br_8^{4+}$ case with terminal Mo–Br and Mo–O bonds of 2.635 and 2.19 Å, respectively. The two waters were staggered with respect to each other and placed so that the resulting molecules of $D_{2d}$ symmetry would correlate with the $O_h$ symmetry model of $Mo_6Br_8^{4+}$. The molecular orbital distribution for those orbitals discussed in the $Mo_6Br_8^{4+}$ case are given in Figure 6 for the $D_{2d}$ case. The net antibonding effect of the terminal ligands on the MO's shown is clearly evident. The $T_{1u}$ and $E_g$ orbitals in particular are raised considerably in the $D_{2d}$ case since these MO's consist primarily of AO's directed at the terminal ligands. The result is a large energy gap of 5.43 eV. Again all of the bonding MO's are filled.

The details of the population analysis will not be given since they parallel those given in Table VIII for the $Mo_6Br_8^{4+}$ calculation except that the Mo–Mo populations are now lower when an AO directed at the terminal ligands is involved. The net overlap populations are interesting as they parallel the observed bond lengths supporting the hypothesis that the differences in Mo–Mo and Mo–Br distances observed are real and result from net bonding effects. The net Mo–Mo overlap populations are 0.337 for $Mo_{11}$–$Mo_{12}$ and 0.344 for $Mo_{11}$–$Mo_{21}$ while the corresponding bond lengths are 2.640 and 2.630 Å, respectively. The Mo–Br overlap populations are 0.309 for $Mo_{11}$–$Br_{21}$, 0.311 for $Mo_{21}$–$Br_{21}$, and 0.392 for $Mo_{11}$–$Br_{11}$; the corresponding bond distances are 2.606, 2.591, and 2.587 Å, respectively.

The bonds formed to the terminal Br ligands are essentially $\sigma$ bonds; for example, the 0.392 overlap population for $Mo_{11}$–$Br_{11}$ has a 0.345 $\sigma$ contribution and a 0.047 $\pi$ contribution. It should be noted that idealized geometries were used so that all of the Mo–Br distances were the same; thus the different overlap populations do not result merely from different bond lengths. We did do a calculation using the actual geometry found with very similar results accentuating the overlap differences. For example, the $Mo_{11}$–$Br_{11}$

(44) A referee has pointed out that there are errors in Table III of the Cotton and Haas[7] paper; certainly this could influence their results.

overlap population at the observed bond length of 2.587 Å is 0.402.

The net atom charges for the various types of atoms are +0.414 for $Mo_{11}$, +0.731 for $Mo_{21}$, −0.629 for $Br_{11}$, −0.082 for $Br_{21}$, −0.938 for $O_{11}$, and +0.483 for H. The $Mo_{21}$ charge could be selectively reduced slightly by choosing VSIP's for oxygen based on the ionization potential of $H_2O$.[45] However, no additional calculations with altered $H_{ii}$'s were done since they would not affect the qualitative effects we were seeking.

The charge distribution and the overlap populations are intimately related and result from the nature of the terminal atoms. The larger the differences in the VSIP's (electronegativities may be used as a rough guide) of the terminal atoms the greater will be the differences in the charges of the equatorial and axial Mo's. In general the Mo atom with the largest charge will be associated with the largest overlap populations and the shortest bonds and *vice versa*. This simple concept is consistent with our calculations and our observed structural parameters; it should have some predictive power with respect to structural parameters of other substituted $Mo_6X_8^{4+}$ clusters.

(45) A. Viste and H. B. Gray, *Inorg. Chem.*, **3**, 1113 (1964).

**Acknowledgments.**—We thank Dr. J. F. Weiher for the magnetic susceptibility measurements and Dr. E. Bromels for his assistance in obtaining the infrared and Raman spectra.

---

CONTRIBUTION FROM THE DEPARTMENT OF CHEMISTRY, MICHIGAN STATE UNIVERSITY, EAST LANSING, MICHIGAN 48823

# Studies on the Chemistry of Halogens and of Polyhalides. XXIX. Complex Compounds of Bromine Chloride

BY TERRY SURLES AND ALEXANDER I. POPOV

*Received January 31, 1969*

Bromine chloride complexes with pyridine, 4-picoline, 2,3- 2,4-, 2,5-, 2,6-, 3,4-, and 3,5-lutidines, and 2,3,6-collidine were prepared. The lutidine complexes, except that of 3,4-lutidine, are quite stable at room temperature under anhydrous conditions. Formation constants of these complexes were determined in carbon tetrachloride solutions. Comparison of these values with the formation constants of iodine(I) chloride and iodine bromide shows that the order of the Lewis acid strength is ICl > IBr > BrCl. Far-infrared spectra of the complexes indicate that the fundamental Br–Cl vibration band is shifted from 430 to 280 $cm^{-1}$ by complexation with pyridine.

## Introduction

While numerous halogen complexes involving iodine, bromine, iodine(I) chloride, iodine(III) chloride, and iodine bromide have been reported in the literature, it is interesting to note that with two exceptions, no mention is made of the compounds of bromine chloride. In 1931, Williams briefly mentioned the preparation of the pyridine–bromine chloride complex,[1] but no details are given on the properties of the resulting compound. More recently, preparation of 4-*n*-amylpyridine–bromine chloride complex was reported by Zingaro and Witmer.[2]

Bromine chloride is a rather unstable compound, and so far, it has not been obtained in the pure state. It is highly dissociated in the vapor phase and in solutions, the equilibrium constant for the reaction $2BrCl \rightleftarrows Br_2 + Cl_2$ being 0.145 at 25° in carbon tetrachloride solutions.[3] This instability of bromine chloride very probably discouraged in the past the investigation of its complexing ability. It should be noted, however, that Scott calculated the electron-accepting ability of bromine chloride (Lewis acid strength) on the basis of the free energy of the formation of trihalide ion $Br_2Cl^-$ in aqueous solutions.[4] On the basis of these calculations, Scott obtained the following order of Lewis acid strengths for the halogens: $ICl \gg BrCl > IBr \gg I_2 > Br_2 \gg Cl_2$.

This work was undertaken in order to study possible formation of bromine chloride complexes with heterocyclic amines and to compare its complexing ability with that of other halogens and interhalogen compounds.

## Experimental Section

**Reagents.**—Technical grade pyridine was refluxed for 2 hr over granulated barium oxide and then slowly distilled through a 100-cm helices-packed column. The middle fraction of the distillate was used.

All of the substituted pyridines used in the investigation were obtained from the Aldrich Chemical Co. These were used without further purification aside from drying. Bromine and chlorine were obtained from J. T. Baker Chemical Co. and Matheson Co., respectively, and were used without further purification.

The purification of carbon tetrachloride has been discussed in previous publications.[5] 1,1,2-Trichlorotrifluoroethane was refluxed for 24 hr over barium oxide and then distilled slowly through a 1-m helices-packed column.[6] 1,2-Dichloroethane was washed successively with sodium bicarbonate solution and water and then dried over calcium sulfate. It was then refluxed for

(1) G. Williams, *J. Chem. Soc.*, 2783 (1931).
(2) R. A. Zingaro and W. B. Witmer, *J. Phys. Chem.*, **64**, 1705 (1960).
(3) A. I. Popov and J. J. Mannion, *J. Am. Chem. Soc.*, **74**, 222 (1952).
(4) R. L. Scott, *ibid.*, **75**, 1550 (1953).
(5) A. I. Popov and W. A. Deskin, *ibid.*, **80**, 2976 (1958).
(6) F. L. Greenwood, *J. Org. Chem.*, **10**, 416 (1945).